Numerical Simulationof Vortex-induced Vibrationfor Segmented Cylinders

Mogan Dhanabalan[1], Nik Mohd Ridzuan Shaharuddin[1,2,*], Farah Ellyza Hashim[1], Mat Hussin Ab Talib[1] and Nik Ahmad Ridhwan Nik Mohd[3]

[1]School of Mechanical Engineering, Faculty of Engineering
Universiti Teknologi Malaysia
81310 UTM Johor Bahru, Johor, Malaysia

[2]Marine Technology Center
Universiti Teknologi Malaysia
81310 UTM Johor Bahru, Johor, Malaysia

[3]Aeronautics Laboratory, School of Mechanical Engineering
Faculty of Engineering
Universiti Teknologi Malaysia
81310 UTM Johor Bahru, Johor, Malaysia

Received: 20 August 2020; Revised: 5 November 2020; Accepted: 30 November 2020; Published: 15 December 2020

ABSTRACT

Vortex-induced vibration (VIV) becomes one of the engineers' main concerns in designing an optimized riser system. Attached segmented buoyancy modules around the riser pipe could be utilized in reducing the VIV through the elimination of the vortex shedding and increasing the riser's fatigue life. However, this can only be achieved if the segmented buoyancy modules are properly arranged along the riser. Thus, this research presents the analysis of vortex-induced vibration of bare and segmented cylinders by using ANSYS FLUENT. The simulation was done in 3D at the stationary condition. For this study, three configuration models, namely, the bare cylinder, 27% segmented cylinder and 46% segmented cylinder were investigated. The simulation also includes grid independency test for the bare cylinder to ensure the results generated were reliable. The turbulent model used in this simulation waslarge eddy simulation (LES), where the vortices created at the back of the cylinder and separation of the flow could be monitored using post-processor. The lift and drag coefficients were simulated by analyzing the flow passes through the cylinder and it was found that the drag coefficientswere reduced by 68.29% and 74.05% for the 27 % and 46% segmented cylinders, respectively in comparison to the bare cylinder's value. Meanwhile, the lift coefficientswere reduced by 24.61% and 44.27% for the 27% and 46% segmented cylinders, respectively, as compared to the bare cylinder counterpart. Both segmented models experience reduction in the drag and lift coefficients where the buoyancy segments disturbed the vortex shedding at downstream.

Keywords: *Computational fluid dynamics,flow around cylinder,large eddy simulation, segmented cylinder,vortex induced vibration*

[*]Corresponding email: nmridzuan@utm.my

1.0 INTRODUCTION

Oil and gas exploration continues to advance into a more profound and harsher environment. To withstand this merging, development engineers and designers faced multiple challenging tasks in developing a practical riser to withstand within the new environment. Continuous and frequent interaction between the riser and the fluid flow causes failure to the structure, mainly due to the vortex-induced vibration (VIV) phenomenon. VIV phenomenon that rises within the interaction between the riser and the sea current has resulted problems involving excessive lift and drag forces on top of fatigue damage or failure to the marine riser itself. Buoyancy modules or segments which are used in giving the extra buoyancy to the marine riser could be utilized in suppressing these problems if it is well arranged with appropriate gap length and buoyancy segment sizes. If a larger diameter of the buoyancy segments is attached to the riser, then it would lead to excessive drag and if it is near to the riser diameter then the suppression will not be effective. Hence an investigation related to buoyancy segments arrangement is essential.

Previous research on the VIV response of pipe with staggered buoyancy segments insights the resulting VIV amplitude for a riser depends on the ratio of the length of buoyancy segments to the size of the gaps between two adjacent buoyancy segments. The existence of buoyancy segments which act as passive device will decrease the fatigue damage rate due to the lower in shedding frequency for its larger diameter than the riser's diameter[1]. It is expected a cylinder fully covered by buoyancy segments of a much larger diameter will vibrate at a lower frequency compared to a bare cylinder with no buoyancy segment. Two different frequencies are excited, and competition exists between lift forces at these two frequencies when a flexible cylinder with both bare and buoyant regions is excited by the same flow.

Numerical simulations are quite common to be conducted in lower subcritical *Reynolds* number range since at the range a relatively thick and laminar boundary layer will be formed, and this might be easier to resolve by the grids. According to Sarpkaya (2004), at high subcritical *Reynolds* number, the turbulent boundary layer held to be thinner than in low *Reynolds* number cases, nearly six times in range[2]. Many previous researchers tend to conduct the simulation in 2D compared to 3D, mainly to reduce the computational cost for the analysis. Dehkordi *et al*.(2011), Derashandeh *et al*. (2014), Tuan (2015) and Asyikin (2012)performed the simulation works using 2D models [3-6]. However, 3D simulations were also carried out by a number of researchers to visualize more effective and real-world analysis on the VIV to design the effective suppression devices.[7-10].

It is essential to have an accurate prediction of the turbulence model as it decides the simulation's accuracy. In general, different numerical methods are used for flow around the fixed cylinder. All *Reynolds*-averaged *Navier–Stokes* (RANS), large eddy simulation (LES) or detached eddy simulation (DES) prediction shows good agreement with experiment studies. However, for the 3-dimensional model analysis, LES plays a significant role as a useful turbulence model. According to Wang *et al*. (2018), large eddy simulation (LES) allows the largest and most important scales of turbulence to be resolved (small eddies are modelled) while significantly reducing the computational cost[10].

The main parameter that defines the configuration of the buoyancy segment is presented in Figure 1. The diameter ratio, D_b/D_r of 5.0 which used by Sukhov (2017) was found to have the lowest drag and lift coefficient value with a diameter of 150 mm and 30 mm for buoyancy module and bare cylinder, respectively[11]. In the present simulation works, the buoyancy segment's diameter is set at 285 mm, which leads to a diameter ratio of 2.5. This diameter ratio has not been studied yet as shown in Table 1. In the same table, the coverage percentage per unit length is also presented. It is noted that most of the

investigations were conducted from 20 – 60%. Hence, the coverage percentage of 27% and 46% are investigated in this simulation works. Meanwhile, for the spacing gap between two adjacent buoyancy segments, Sukhov (2017) used 150 mm and 300 mm of the spacing gap, which give spacing ratio L_c/L_b of 1 and 2, respectively[11]. Hence, the spacing gap of 273 mm and 819 mm which correspond to L_c/L_b of 1 and 3, respectively, were used in this study.

Based on the literature study, it was learned that there are a number of diameter ratios, spacing ratio and coverage percentage that have been utilized in investigating the effectiveness of VIV suppression using buoyancy modules, and it is still in an open area for further investigation. Hence, this paper aims to examine the lift, drag and flow around a stationary cylinder with and without the buoyancy modules at different diameter ratios and coverage areas. It is important to note that this study provides the basic or fundamental results of the buoyance segment arrangement towards lift and drag responses.

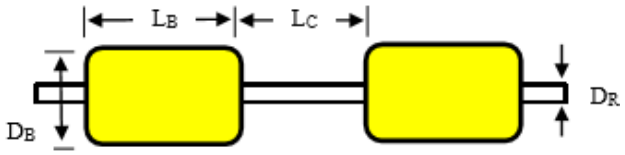

Figure 1: Definition of the gap and buoyancy segment lengths[12]

Table 1: Buoyancy segment coverage percentage used by previous experimental works

Author	Mode	D_b (mm)	L_b (mm)	D_b/D_r	L_c/L_b	Coverage percentage (%)
Sukhov [11]	Experiment	150	150	5	1.0 and 2.0	20-60
Zhibiao *et al*. [12]	Experiment	80	400	30	1.0, 2.0 and 3.0	20-80
Cao and Cheng [13]	Experiment	135.5	148	4.8	2.3	40-60
Wu *et al*. [14]	Experiment	80	400	30	0.5, 1.0. 1.5 and 2.5	20-100
Jhingran *et al*.[15]	Experiment and Simulation	150	150	30	1.0 and 2.0	20-60

2.0 NUMERICAL MODELS

2.1 Large Eddy Simulation (LES)

By numerically solving the unsteady incompressible *Navier-Strokes* equations, the flow around the cylinder was calculated, LES was used to solve turbulent flow [7].

$$\frac{\partial \bar{u}_i}{\partial t} + \frac{\partial}{\partial t_j}\bar{u}_i\bar{u}_j = -\frac{1}{\rho}\frac{\partial \bar{p}_i}{\partial x_j} + \upsilon\frac{\partial \bar{u}_i}{\partial x_i \partial x_j} - \frac{\partial \tau_{ij}}{\partial x_i} \quad (1)$$

where the sub grid stresses are given by:

$$\tau_{ij} = \overline{u_i u_j} - \bar{u}_i\bar{u}_j \quad (2)$$

with the *smagorinsky* sub grid scale turbulence model:

$$\tau_{ij} = 2\boldsymbol{\nu T} S_{ij} \quad (3)$$

$$\nu T = (\mathrm{Cs}\,\Delta)2\sqrt{\mathbf{2}\bar{Sij}\,\bar{Sij}} \quad (4)$$

The local strain rate tensor $\bar{Sij}$ is defined as:

$$\bar{S}_{ij} = \frac{1}{2}\left(\frac{\partial \bar{u}_i}{\partial x_j} + \frac{\partial \bar{u}_j}{\partial x_i}\right) \quad (5)$$

and the filter width is taken as the local grid size, for example:

$$\Delta = (\Delta_x \Delta_y \Delta_z)^{1/3} \quad (6)$$

3.0 SIMULATION SETUP AND VALIDATION

3.1 Building 3D Model and Meshing

The model was designed through the Design Modeler package in ANSYS 2020 R1 student version. Particulars on the cylinder and buoyancy module sizes are shown in Table 2. Meanwhile, Figures 2(a) to 2(c) show the bare cylinder, 27 % and 46 % of segmented buoyance modules, respectively. A rectangular domain with length, width and depth of 40*D*× 20*D*× 3 m, respectively,where *D* is the diameter of the cylinder is used in this simulation, respectively. The center of the model cylinder is located at 10*D* from the inlet section and 10*D* from the domain's sidewall. This domain size is sufficient as the wall effect is minimized without jeopardizing the computation time due to the large number of meshing elements.

Table 2: Model specifications for bare cylinder and buoyancy module segments

Specification	Bare cylinder	Buoyancy segments
Diameter Cylinder (*D*)	114 mm	285 mm
Length (*L*)	3000 mm	273 mm
D_b/D_r	-	2.5
Spacing ratio		3 and 1
Number of modules		3 and 5
Coverage (%)		27 and 46

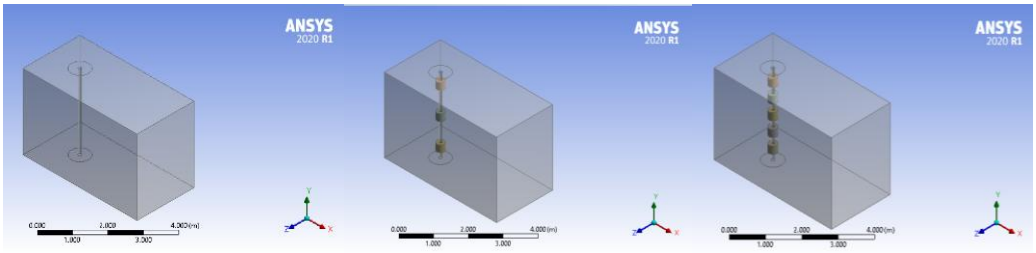

(a) (b) (c)

Figure 2: 3D models for (a) bare (b) 27% segmented (c) 46% segmented cylinders in rectangular domain

As the domain size is defined, mesh will be generated within the solution domain as shown in Figures 3(a) to 3(c). The mesh is determined based on the discrete location where the calculation is executed. Hexahedron meshing is the standard type of meshing applied in 3D meshing. The quality of meshing is essential to get the most precise results.

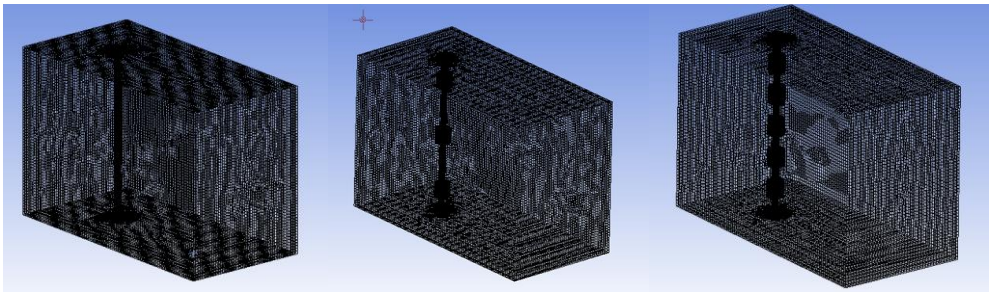

(a) (b) (c)

Figure 3: Meshed 3D models for (a) bare (b) 27% segmented (c) 46% segmented cylinders in rectangular domain

3.2 Simulation Setup

The boundary type is usually defined for the analysis of each model to be done. ANSYS FLUENT provides information on the flow condition at the boundaries of the physical model. The boundary types can be defined as inlet, outlet, cylinder as well as no-slip condition. Symmetry boundary is also applied to the model since it consists of top, bottom and two more sidewalls. The simulation setting used in the project is summarized in Table 3.

Table 3: Simulation settings

Simulation type	3D, Unsteady
Solver	Double precision, Pressure based and implicit
Temporal discretization	2nd order
Turbulence model	LES model
Pressure	Standard
Pressure velocity coupling	SIMPLE
Inlet	Velocity Inlet
Outlet	Pressure outlet
Top, Bottom, side wall	Symmetry
Cylinder wall	No slip wall

3.2 Grid Independency Test

The grid independency test of the bare cylinder is carried out in this study to determine whether the simulation results are reliable despite the number of mesh elements used. Mesh resolution ranging from 350,000 to 500,000 at the same inlet velocity was simulated. Figure 4 shows the lift and drag coefficient values against the number of elements. It can be seen that the values for the drag and lift coefficients are constant for Case C and D as shown in Table 4. Hence,the number of meshing for case C was used for all simulation works.

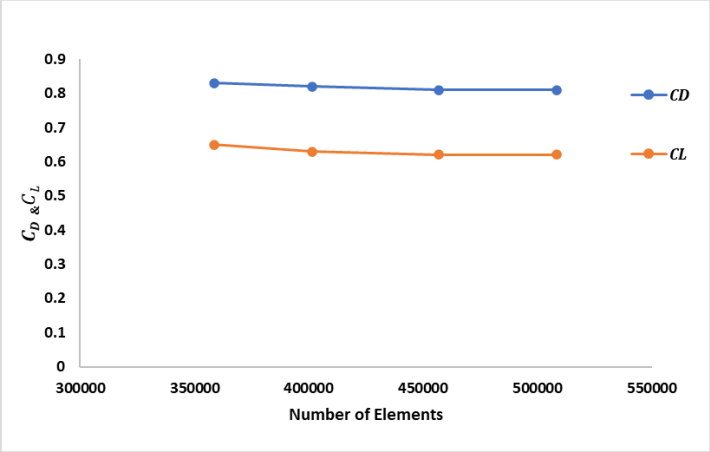

Figure 4: Grid independency test for different number of elements

Table 4: Meshing cases setting for the project

CASE	Mesh size (number of elements)	C_D	C_L
A	358535	0.83	0.65
B	401639	0.82	0.63
C	456860	0.81	0.62
D	508482	0.81	0.62

3.3 Validation Test

It is vital to validate the results with previous work to ensure a similar result is achieved. For this particular case, works by Wang *et al*. (2018) have been selected as it also deals with the 3D simulation of VIV study for a rigid cylinder with static meshing[10]. Figures 5(a) and (b) show the result of the present study against those in [10] for the lift and drag coefficients. It can be seen that the present study result is in agreement with previous work except that the amplitudes for both lift and drag are not the same due to different diameter used for the simulation works. The diameter used in [10] is 300 mm which leads to bigger lift and drag coefficients as compared to the current simulation works.

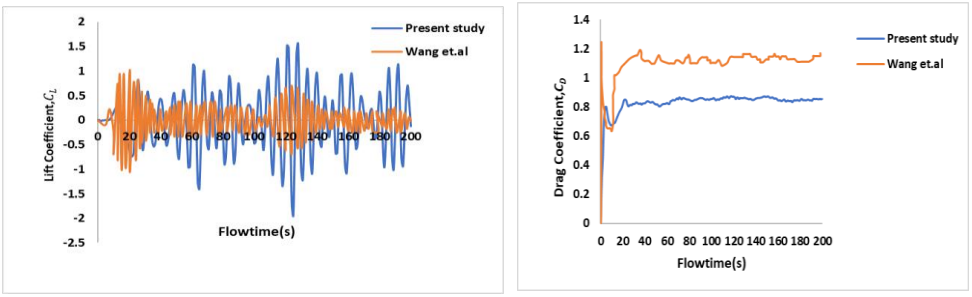

(a) (b)

Figure 5: 3D simulation results for validation (a) lift coefficient and (b) drag coefficient

4.0 RESULTS AND DISCUSSION

4.1 Numerical Simulation Flow

The numerical simulation was conducted for all geometries, including the bare cylinder and segmented ones with different coverage percentages, which are 27% and 46%. The simulation's objective is to determine the effectiveness of the buoyancy modules in

reducing the VIV and determine for which coverage the VIV can be encountered more effectively. From the validation study conducted on the bare cylinder, the flow around the bare cylinder was presented. The selected reduced speed was at U_r = 5 since it comparatively shows large shedding effect and lift coefficient compared to other reduced speeds.The reduced speed is non-dimensional which is defined by $Ur = V/f_nD$ where V is the velocity of the fluid in m/s, and f_n is the natural frequency the cylinder at 0.7 Hz.

4.2 Flow Visualization: Bare Cylinder

In this section, the simulation was carried out with a bare cylinder with several reduced speeds ranging from 4 to 10. The simulation results, such as the velocity magnitude contour and the vorticity magnitude contour, are shown in Figures 6 and 7for flow at 150 s.

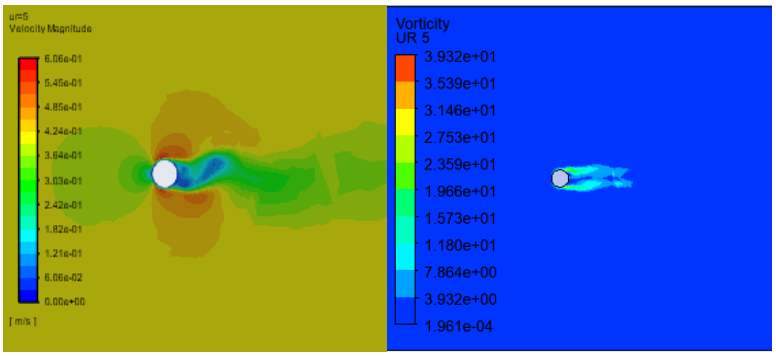

(a) (b)

Figure 6: Top views showing (a) velocity and (b)vorticity magnitude contour of bare cylinder at $U_r = 5$

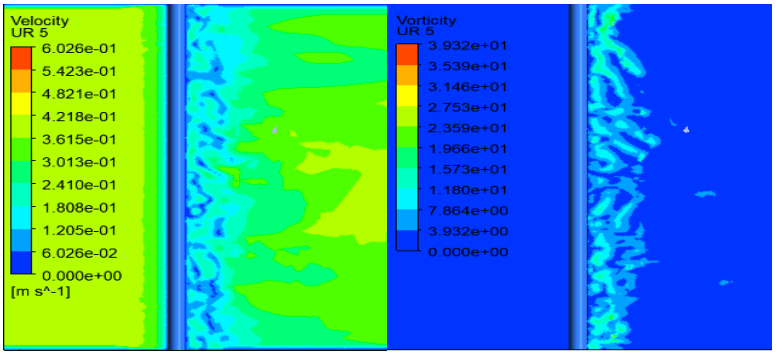

(a) (b)

Figure 7: Side views showing (a) velocity and (b)vorticity magnitude contour of bare cylinder at $U_r = 5$

4.3 Flow Visualization: 27% and 46% Segmented Cylinders

This section will show the results on the segmented cylinder with different coverage of buoyancy modules, which are 27% and 46%. In order to present the top view of the segmented cylinder, the domain was slice at two different sections. The first section was bare cylinder and the second section was the buoyancy segment. Figures 8 and 9 show the velocity magnitude contour and the vorticity magnitude contour for 27% and 46% of the segmented cylinder. It can be seen that larger vortices were formed by the buoyancy module and affected the vortices produced by region without the buoyancy module.

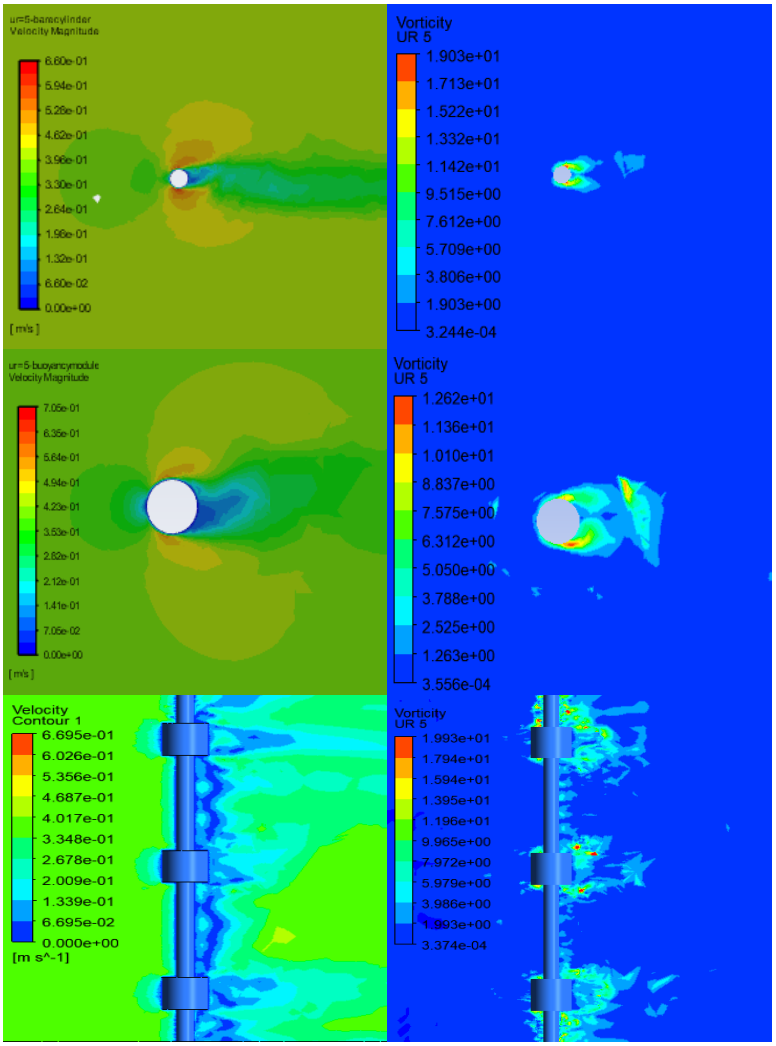

Figure 8: Velocities and vorticity magnitude contours for 27% segmented cylinder

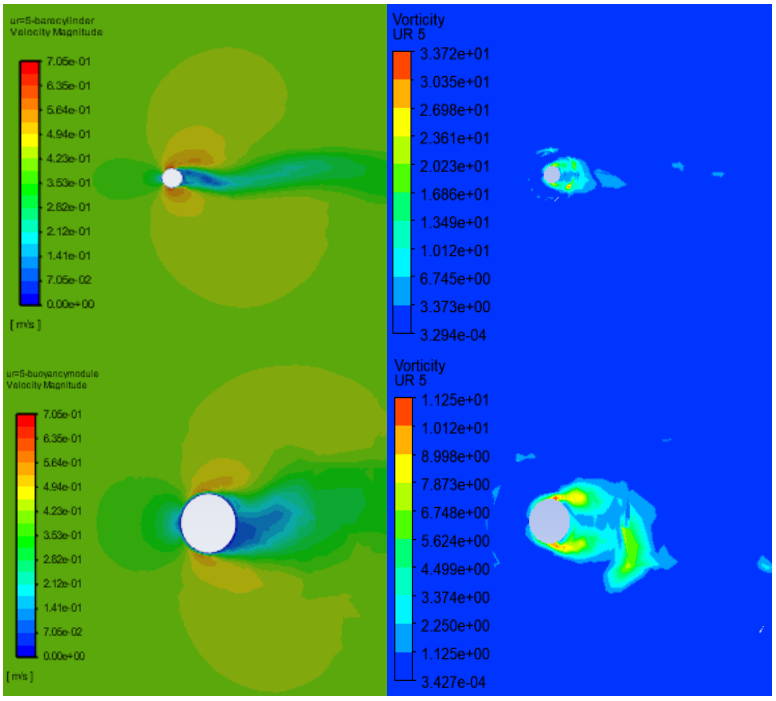

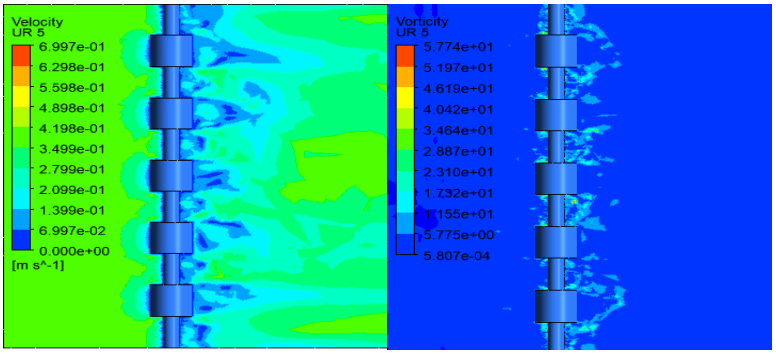

Figure 9: Velocities and vorticity magnitude contours for 46% segmented cylinder

4.4 Analysis of VIV Bare and Different Coverage Segmented Cylinders

The present simulation study shows a segmented cylinder's effect on the formation of vortex shedding on flow past a circular cylinder. To be more specific, the analysis results will focus more on U_r= 5for both bare and segmented cylinders since there is an excitation in the value of lift coefficient at this particular reduced speed, as shown in Figure 10. Figure 10 shows the root mean squared (rms) of the lift coefficient for the bare and segmented cylinders. The graph indicates that the rms lift coefficient value is decreased when the coverage percentage of the buoyancy modules increases from none to 27% and 46%. The lift coefficient value at U_r= 5for the bare cylinder is 0.759, whereas for the segmented cylinder with 27% and 46% coverage of the segmented cylinders show the lift coefficient values of 0.209 and 0.171, respectively. Figure 11 shows the percentage of reduction of the rms lift coefficient for bare and segmented cylinders (percentage-wise). Comparatively, 46% of segmented cylinders experience more lift coefficient reduction than 27% of the segmented cylinder, where each configuration shows reduction of 74.60% and 68.29%, respectively, at a reduced velocity of U_r= 5.

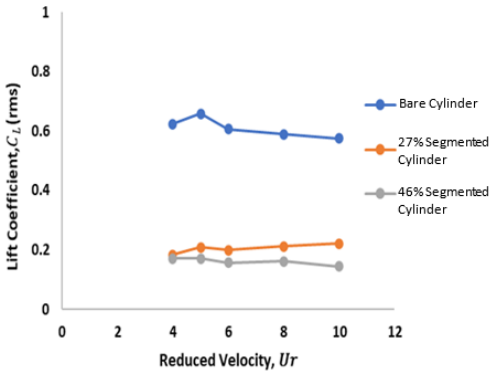

Figure 10: Lift coefficient, C_L response for bare and segmented cylinders

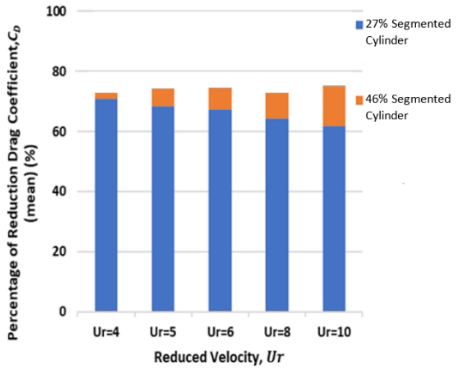

Figure 11: Percentage of reduction of lift coefficient for segmented cylinders

Figure 12 shows the mean drag coefficient (C_D) for bare and segmented cylinders. The mean drag coefficient for the bare cylinder is 0.829, whereas the segmented cylinder with 27% and 46% coverage of buoyancy modules show $C_D$as 0.625 and 0.462, respectively. The mean drag coefficient is reduced using segmented modules. Figure 13 represents the percentage of reduction of drag coefficient, C_D (mean) of bare and segmented cylinders. Comparatively, 46% of segmented cylinders experience more reduction in drag coefficient than 27% of the segmented cylinder, where each configuration shows 24.61% and 44.27% respectively at reduced velocity of U_r= 5. Generally, for all reduced speed, it shows a similar trend on the drag reduction results.

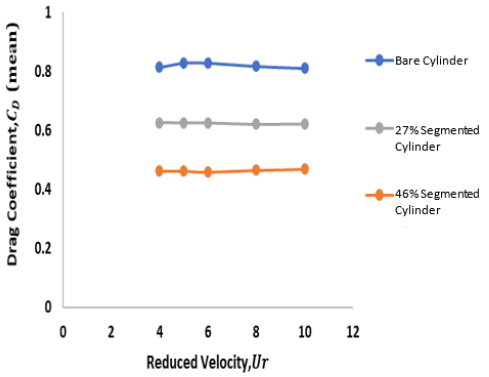

Figure 12: Drag coefficient, $C_D$response for bare and segmented cylinders

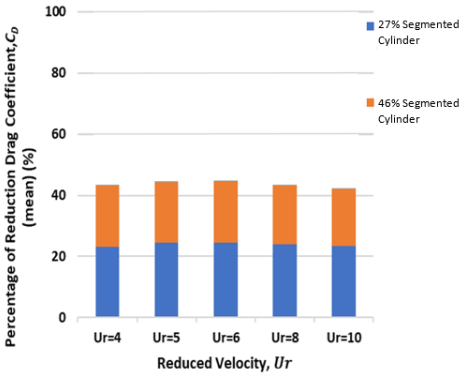

Figure 13: Percentage of reduction of drag coefficient for segmented cylinders

5.0 CONCLUSION

The effects of diameter and spacing ratio, which lead to two different cylinder coverages, were investigated in this research. Generally, the results obtained show that the existence of the buoyancy modules could reduce the VIV by looking at the reduction of the lift coefficient of the segmented body compared with the bare cylinder. Two different coverages were investigated. It was found that the lift coefficient for the 46% of buoyancy module coverage lead to extra suppression compared with the 27% of buoyancy module coverage, where each configuration shows 74.60% and 68.29% suppression level, respectively at a reduced velocity of U_r= 5. This suppression is due to large vortices generated from the buoyancy modules which interrupt the region without the buoyancy modules or vice versa. Besides, it was found that the drag coefficient was also reduced as more buoyancy modules were attached. Hence, proper selection of the diameter and spacing ratio of buoyancy modules could suppress the VIV.

ACKNOWLEDGMENTS

The authors would like to acknowledge the Ministry of Higher Education Malaysia for funding this research via the Fundamental Research Grant Scheme (FRGS), Grant No 5F129 and the Universiti Teknologi Malaysia (UTM) for providing the infrastructure, facility and support.

REFERENCES

1. Shaharuddin N.M.R. and Mat Darus I. Z., 2018. Implementation of Active Control on Flexibly Mounted Pipe Exposed to Vortex Induced Vibration using Rotating Rod, *Meccanica*, 53: 2091–2103. doi:10.1007/s11012-017-0797-8.
2. Sarpkaya T., 2004. A Critical Review of the Intrinsic Nature of Vortex Induced Vibrations,*J Fluid Strut*,19(4): 389-447. doi:10.1016/j.jfluidstructs.2004.02.005.
3. DehkordiB.G., Moghaddam H.S.and JafariH.H., 2011. Numerical Simulation of Flow over Two Circular Cylinders in Tandem Arrangement, *J Hydrodyn,Ser. B*, 23(1): 114-126. doi:10.1016/S1001-6058(10)60095-9.
4. DerakshandehJ.F., ArjomandiM., DallyB. and CazzolatoB., 2014. The Effect of Arrangement of Two Circular Cylinders on the Maximum Efficiency of Vortex Induced Vibration Power using a Scale-adaptive Simulation Model, *J Fluid Strut*, 49: 654-666. doi:10.1016/j.jfluidstructs.2014.06.005.
5. TuanL.N.T., 2015.*Vortex and Wake Induced Vibration in an Array of Cylinders*, Phd Thesis, University of Southampton.
6. AsyikinM.T., 2012.*CFD Simulation of Vortex Induced Vibration of a Cylindrical Structure*, Master Thesis, Norwegian University of Science and Technology.

7. MalikA.M.A., TofaM.M., SaeedY.A. and AbynJ.H., 2014. Experimental and Numerical Studies of Vortex Induced Vibration on Cylinder, *J Teknol*, 66(2): 169-175. doi:10.11113/jt.v.2014.66.2512.
8. DineshT.M., 2019. *Numerical Analysis of Marine Riser Vortex-Induced Vibration with Helical Strake Suppression Device*, Master Thesis,University of Malaya.
9. Kitagawa T.and OhtaH., 2008. Numerical Investigation on Flow Around Circular Cylinder in Tandem Arrangement at a Subcritical Reynolds Number, *J Fluid Strut*, 24: 680-699. doi:10.1016/j.jfluidstructs.2008.10.010.
10. WangC., SunM., ShankarK., Xing S. and ZhangL., 2018. CFD Simulation of Vortex Induced Vibration for FRP composite Riser with Different Modelling Methods, *Appl. Sci.*, 8(5): 684. doi:0.3390/app8050684.
11. Sukhov A.,2017. *VIV Prediction of Steel Lazy Wave Riser*, Master Thesis, Faculty of Science and Technology, University of Stavanger.
12. Zhibiao R., Vandiver J.K. and Jhingran V., 2013. VIV Excitation Competition Between Bare and Buoyant Segments of Flexible Cylinders, *Procs of International Conference on Ocean, Offshore and Arctic Engineering*. doi: 10.1115/OMAE2013-11296
13. Cao P. and ChengJ., 2013. Design of Steel Lazy Wave Riser for Disconnectable FPSO,*Procs of Offshore Technology Conference*. doi: 10.4043/24166-MS
14. WuJ., Reddy L.M. and ChenO.M., 2016.Prediction of Riser VIV with Staggered Buoyancy Elements,*Procs ofInternational Conference on Ocean, Offshore and Arctic Engineering*. doi: 10.1115/OMAE2016-54502
15. JhingranV., ZhangH., LieH., Braaten H.cand VandiverJ.K., 2012. Buoyancy Spacing Implications for Fatigue Damage Due to Vortex-induced Vibrations on a Steel Lazy Wave Riser (SLWR),*Procs. of Offshore Technology Conference*. doi: 10.4043/23672-MS